Wideband Dielectric Resonator Antenna With a Tunnel

Tze-Hsuan Chang, *Student Member, IEEE*, Yu-Ching Huang, Wei-Fang Su, and Jean-Fu Kiang, *Member, IEEE*

***Abstract*—A wideband rectangular dielectric resonator (DR) with a horizontal tunnel is proposed. The bandwidth of the TE^{y}_{111} mode is increased by using the tunnel to reduce the Q-factor of the DR. As the tunnel height is increased, the electric field distribution of the TE^{y}_{112} mode is significantly modified such that its electric field distribution near the top surface of DR is similar to that of the TE^{y}_{111} mode, rendering a broadside radiation pattern. The band of the modified TE^{y}_{112} mode is merged with that of the TE^{y}_{111} mode to achieve a wide bandwidth of 20% (4.76–5.86 GHz) with broadside radiation pattern of vertical polarization on the xy-plane. The proposed DR antenna can be used in WLAN 802.11a applications.**

***Index Terms*—Dielectric resonator (DR), resonant mode.**

I. Introduction

DUE TO negligible ohmic loss, dielectric resonators can be used to design high-efficiency antennas, and many efforts have been devoted to increase their bandwidth. Broadband characteristics of a dielectric resonator (DR) can be achieved by stacking several cylindrical, circular, triangular, or elliptic DRs of different sizes to merge their resonant bands [1]–[4]. Structural discontinuities in DRs tend to reduce their Q factor. For example, a circular or an elliptical DR with a cylindrical hole filled with low-permittivity material renders a wide bandwidth [5]. Inserting an air gap between the ground plane and the DR is equivalent to creating discontinuities within the DR, hence can increase its impedance bandwidth [6], [7].

By increasing the ratio of inner to outer radii of dielectric ring resonators, the stored energy can be dissipated at a higher rate, thus reducing the Q factor [8]. In [9], a rectangular DR with a notch carved at bottom is proposed. This DR and its image with respect to the ground plane form a rectangular dielectric ring, achieving a wider impedance bandwidth than its intact counterpart.

The radiation pattern of a DR is determined by the electric field distribution on the DR surface. Hence, dual-band and wideband characteristics can be attained by exciting proper modes with similar electric field distributions on the DR surface [10].

In this work, a horizontal tunnel is drilled off a rectangular DR to reduce its Q factor and hence increase its impedance bandwidth. Increasing the tunnel height will significantly modify the electric field distribution of the TE^{y}_{112} mode on the top surface of the DR, rendering a broadside radiation pattern similar to that of the TE^{y}_{111} mode. By adjusting the dimensions of the tunnel, the bands of the TE^{y}_{111} mode and the modified TE^{y}_{112} mode can be merged to form a wider band.

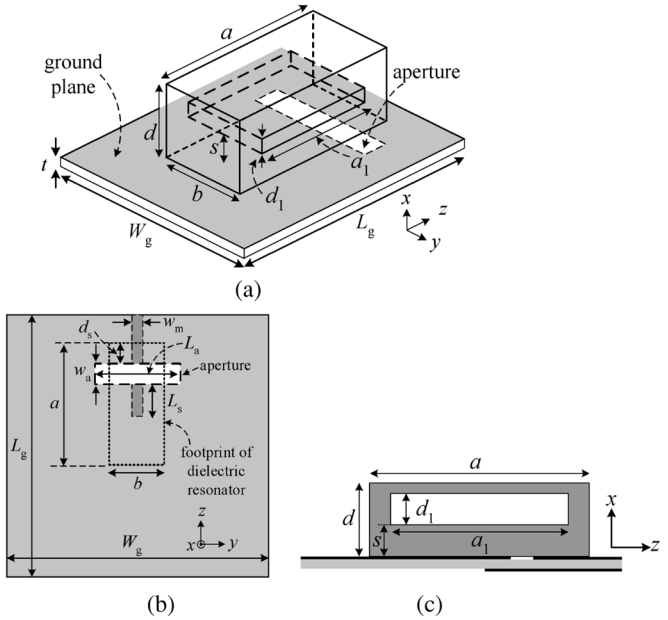

Fig. 1. Configuration of DR with a horizontal tunnel: (a) panoramic view, (b) layout of feeding structure, and (c) side view.

II. Resonant Modes

Fig. 1 shows the configuration of the proposed DR with a tunnel, the latter is used to modify the electric field distribution and reduce the Q factor of DR. The tunnel has dimensions of $a_1 \times b \times d_1$, and is offset from the ground plane by s. The effect of tunnel on the resonant frequency will be analyzed first. Consider an intact DR of dimensions $a \times b \times d$, placed on a ground plane. The field distribution of the TE^{y}_{111} mode inside the intact DR can be expressed as

$$\begin{aligned}
E_{0x} &= -k_z A \cos(k_x x)\cos(k_y y)\sin(k_z z)\\
E_{0y} &= 0\\
E_{0z} &= k_x A \sin(k_x x)\cos(k_y y)\cos(k_z z)\\
H_{0x} &= \frac{k_x k_y}{j\omega\mu} A \sin(k_x x)\sin(k_y y)\cos(k_z z)\\
H_{0y} &= \frac{k_x^2 + k_z^2}{j\omega\mu} A \cos(k_x x)\cos(k_y y)\cos(k_z z)\\
H_{0z} &= \frac{k_z k_y}{j\omega\mu} A \cos(k_x x)\sin(k_y y)\sin(k_z z) \qquad (1)
\end{aligned}$$

Manuscript received March 29, 2007; revised March 27, 2008. This work was supported by the National Science Council, Taiwan, ROC, under Contract NSC 93-2213-E-002-034.

T.-H. Chang and J.-F. Kiang are with the Department of Electrical Engineering and the Graduate Institute of Communication Engineering, National Taiwan University, Taipei, Taiwan. R.O.C. (e-mail: jfkiang@cc.ee.ntu.edu.tw).

Y.-C. Huang and W.-F. Su are with the Department of Materials Science and Engineering, National Taiwan University, Taipei, Taiwan, R.O.C.

Digital Object Identifier 10.1109/LAWP.2008.928477

where A is an arbitrary constant, $k_x = \pi/2d, k_z = \pi/a$, and k_y is obtained by solving [11]

$$\frac{k_y b}{2} = \tan^{-1}\left(\frac{\sqrt{k_x^2 + k_z^2}}{k_y}\right). \tag{2}$$

The resonant frequency can then be determined as

$$f_r = \frac{c}{\sqrt{\epsilon_r}}\sqrt{k_x^2 + k_y^2 + k_z^2}. \tag{3}$$

The field distribution of the TE^y_{112} mode inside an intact DR can be expressed as

$$\begin{aligned}
E_{0x} &= k_z B\cos(k_x x)\cos(k_y y)\cos(k_z z)\\
E_{0y} &= 0\\
E_{0z} &= k_x B\sin(k_x x)\cos(k_y y)\sin(k_z z)\\
H_{0x} &= \frac{k_x k_y}{j\omega\mu} B\sin(k_x x)\sin(k_y y)\sin(k_z z)\\
H_{0y} &= \frac{k_x^2 + k_z^2}{j\omega\mu} B\cos(k_x x)\cos(k_y y)\sin(k_z z)\\
H_{0z} &= \frac{-k_z k_y}{j\omega\mu} B\cos(k_x x)\sin(k_y y)\cos(k_z z)
\end{aligned} \tag{4}$$

where B is an arbitrary constant, $k_x = \pi/2d, k_z = 2\pi/a, k_y$ and the resonant frequency can be determined from (2) and (3), respectively.

If a narrow tunnel is drilled off the intact DR, the original space occupied by the latter remains the same except the permittivity distribution becomes space dependent as $\epsilon(\bar{r})$. The field distribution of the TE^y_{111} mode inside the tunnel can be approximated as

$$\begin{aligned}
E_x &= -k_z m_1 A\cos(k_x s)\cos(k_y y)\sin(k_z z)\\
E_y &= 0\\
E_z &= k_x A\sin(k_x s)\cos(k_y y)\cos(k_z z)\\
\bar{H} &= \bar{H}_0
\end{aligned} \tag{5}$$

where m_1 is a magnifying factor. Similarly, the field distribution of the TE^y_{112} mode inside the tunnel can be approximated as

$$\begin{aligned}
E_x &= k_z m_2 B\cos(k_x s)\cos(k_y y)\cos(k_z z)\\
E_y &= 0\\
E_z &= k_x B\sin(k_x s)\cos(k_y y)\sin(k_z z)\\
\bar{H} &= \bar{H}_0
\end{aligned} \tag{6}$$

where m_2 is another magnifying factor. The magnifying factors m_1 and m_2 are determined by observing the electric field distributions simulated with HFSS.

TABLE I
EFFECT OF TUNNEL HEIGHT d_1 ON RESONANT FREQUENCY f_r (GHZ)

d_1 (mm)	0.1	0.3	0.5	1
TE^y_{111}				
Δf_r (Eq. (7))	0.083	0.174	0.23	0.35
Δf_r/BW (HFSS)	0.08/5.1	0.18/0.6	0.28/8	0.4/7.5
TE^y_{112}				
Δf_r (Eq. (7))	0.19	0.38	0.45	0.54
Δf_r/BW (HFSS)	0.18/4.3	0.4/4.5	0.54/4	0.7/-

Parameters (mm): $s = 3$, $d_s = 7$, $L_a = 13$, $L_s = 6$, $a = 21$, $b = 7$, $d = 7$, $a_1 = 16$, $w_a = 1$, $W_g = L_g = 50$.

Let $(\bar{E}_0, \bar{H}_0)$ and $(\bar{E}, \bar{H})$ be the field distributions of the TE^y mode without and with the tunnel, respectively, ω_0 and ω be the resonant frequencies of the TE^y mode without and with the tunnel, respectively. The resonant frequency of the DR with tunnel can be approximated as

$$\omega = \frac{\tilde{W}_m + \tilde{W}_{eb}}{\tilde{W}_m + \tilde{W}_{ea}}\omega_0 - \frac{j\iint_S \left(\bar{H}\times\bar{E}_0^* + \bar{H}_0^*\times\bar{E}\right)\cdot d\bar{s}}{\tilde{W}_m + \tilde{W}_{ea}} \tag{7}$$

with

$$\tilde{W}_m = \iiint_V \mu\bar{H}_0^*\cdot\bar{H}dv$$

$$\tilde{W}_{ea} = \iiint_V \epsilon(\bar{r})\bar{E}\cdot\bar{E}_0^* dv, \tilde{W}_{eb} = \iiint_V \epsilon_r\epsilon_0\bar{E}_0^*\cdot\bar{E}dv$$

where V is the space occupied by the intact DR with surface S. Substituting (5) and (6) into (7), the shift in resonant frequencies can be estimated.

Table I summarizes the effect of tunnel height d_1 on the shift of resonant frequencies by using HFSS simulation and analysis, respectively. The resonant frequencies of both the TE^y_{111} and TE^y_{112} modes increase as the tunnel height increases. The shift of resonant frequencies by both approaches matches well as the tunnel is thin.

As the tunnel becomes thicker, the electric field in the tunnel can no longer be approximated as the original electric field magnified by a factor, as in (5) and (6). Equations (1) and (4) also become inaccurate in describing the field in the DR. The HFSS is then used to determine the tunnel effect when the tunnel becomes thick.

Fig. 2 shows the effect of tunnel height d_1 on the resonant frequencies of TE^y_{111} and TE^y_{112} modes. When the tunnel is thin, the electric field distribution of the TE^y_{111} mode is roughly parallel to the tunnel width as shown in Fig. 3(a), while the E_x component of the TE^y_{112} mode is significantly enhanced in the tunnel as shown in Fig. 3(b). The resonant frequencies of TE^y_{111} and TE^y_{112} modes increase as d_1 is increased, so does the impedance bandwidth. As the tunnel height is further increased to greater than 1 mm, the electric field distribution of

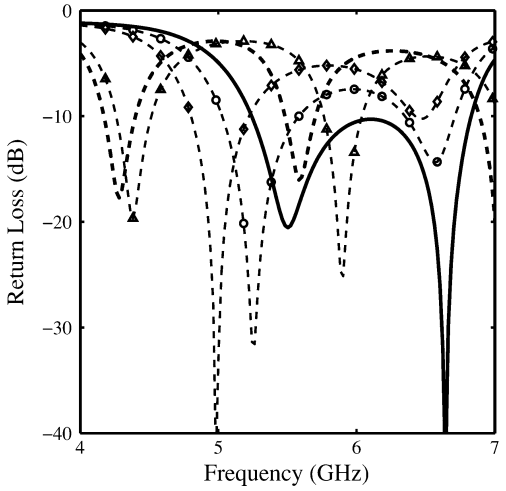

Fig. 2. Effect of tunnel height d_1 on resonant frequencies of the TE^y_{111} and TE^y_{112} modes, $a = 21$ mm, $d = 7$ mm, $b = 6$ mm, $a_1 = 16$ mm, $s = 3.3$ mm, $\epsilon_r = 20, w_a = 2$ mm, $d_s = 7$ mm, $L_a = 11$ mm, $L_s = 8$ mm, $W_g = L_g = 50$ mm, $t = 0.6$ mm, - - - : $d_1 = 0.1$ mm, -△- : $d_1 = 0.5$ mm, -◇- : $d_1 = 1$ mm, -○- : $d_1 = 2$ mm,—: $d_1 = 2.9$ mm.

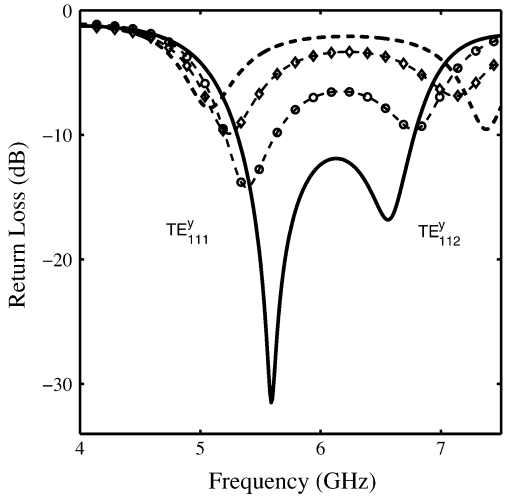

Fig. 4. Effect of tunnel offset s on resonant frequencies of the TE^y_{111} and TE^y_{112} modes, $a = 21$ mm, $b = 6$ mm, $d = 7$ mm, $a_1 = 16$ mm, $d_1 = 3$ mm, $\epsilon_r = 20, w_a = 2$ mm, $d_s = 6$ mm, $L_a = 11$ mm, $L_s = 8$ mm, $W_g = L_g = 50$ mm, $t = 0.6$ mm, - - - : $s = 1.5$ mm, -◇- : $s = 2$ mm, -○- : $s = 2.5$ mm, - - - : $s = 3$ mm.

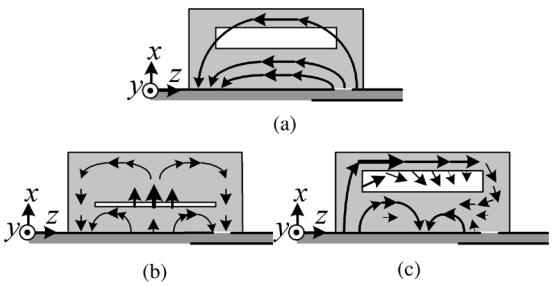

Fig. 3. Electric field distribution of (a) TE^y_{111} mode, (b) TE^y_{112} mode with thin tunnel, and (c) TE^y_{112} mode with thick tunnel.

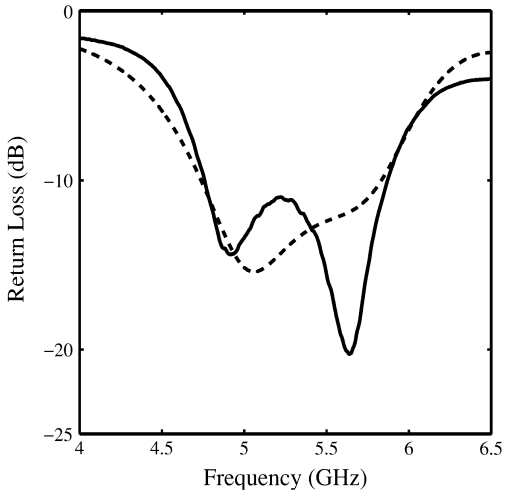

Fig. 5. Return loss of DR with tunnel,–: measurement, - - -: simulation, $a = 21.2$ mm, $d = 7.25$ mm, $b = 7.7$ mm, $d_1 = 2.9$mm, $a_1 = 16$ mm, $s = 3.3$ mm, $\epsilon_r = 21, w_a = 2$ mm, $d_s = 7.2$ mm, $L_a = 13$ mm, $L_s = 8$ mm, $W_g = L_g = 70$ mm, $t = 0.6$ mm.

the TE^y_{112} mode is significantly modified, with its E_z component on the top surface of the DR similar to that of the TE^y_{111} mode, as shown in Fig. 3(c). Hence, this mode will provide similar broadside radiation pattern on the xy-plane. Note that the bands of the TE^y_{111} mode and the modified TE^y_{112} mode merge at $d_1 = 2.9$ mm.

Note that when the tunnel is thin ($d_1 \leq 0.1$ mm), the magnifying factors m_1 and m_2 are very close to ϵ_r. As the tunnel becomes thicker, m_1 and m_2 begin to deviate from ϵ_r, and the simulated electric field distributions are used to estimate the magnifying factors. When the tunnel height d_1 is greater than 1 mm, the field distribution becomes complicated that even the functional forms in (5) and (6) become inaccurate.

The TE^y_{111} mode has a strong E_z component near the top surface of DR, while the TE^y_{112} mode has a strong E_x component near the ground. Hence, changing the tunnel position will adjust the characteristics of both TE^y_{111} and TE^y_{112} modes. Fig. 4 shows the effect of tunnel offset s on the resonant frequencies with $d_1 = 3$ mm. As s increases, the resonant frequency of TE^y_{111} mode is increased, while that of the modified TE^y_{112} mode is decreased. The bands of the TE^y_{111} and the modified TE^y_{112} modes merge to form a wide bandwidth at $s = 3$ mm.

III. Results and Discussions

As shown in Fig. 1, the DR antenna is fed by a microstrip line through an aperture of size $w_a \times L_a$ on the ground plane of size $W_g \times L_g$, the offset between the DR and the aperture is d_s. The microstrip line is extended over the aperture by L_s, fabricated on an FR4 substrate with $\epsilon_r = 4.4$ and of thickness t.

With proper tunnel dimensions, the bands of the TE^y_{111} and the modified TE^y_{112} modes merge. By tuning the DR position d_s, the length of aperture L_a, and the length of microstrip extension L_s, the input impedance can be better matched. Fig. 5 shows the measured and simulated return loss, their band edges match reasonably well. The 10-dB impedance bandwidth is 20% (4.76–5.86 GHz), well covers the WLAN 802.11a band (5.15–5.85 GHz). The minima of the return loss are contributed by the TE^y_{111} and the modified TE^y_{112} modes, respectively.

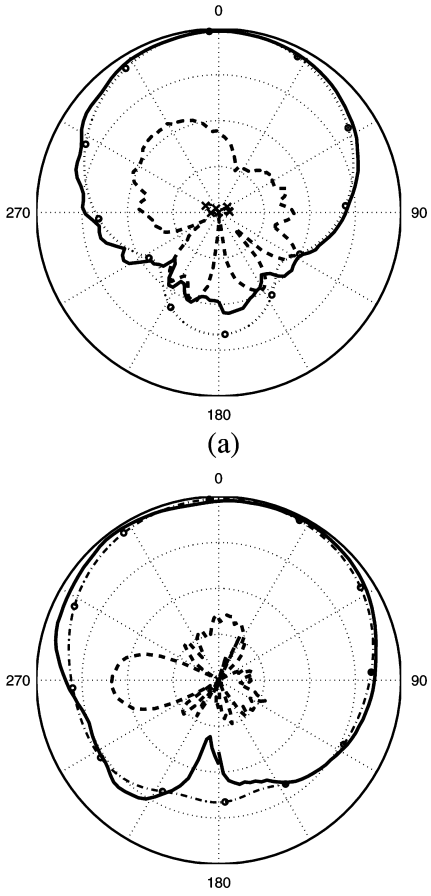

Fig. 6. Radiation pattern at 4.98 GH, (a) xy-plane, (b) xz-plane, - - -: measured E_θ, - - -: measured E_ϕ, -×-: simulated E_ϕ, -o-: simulated E_θ, 10-dB per division on radials, all parameters are the same as in Fig. 5.

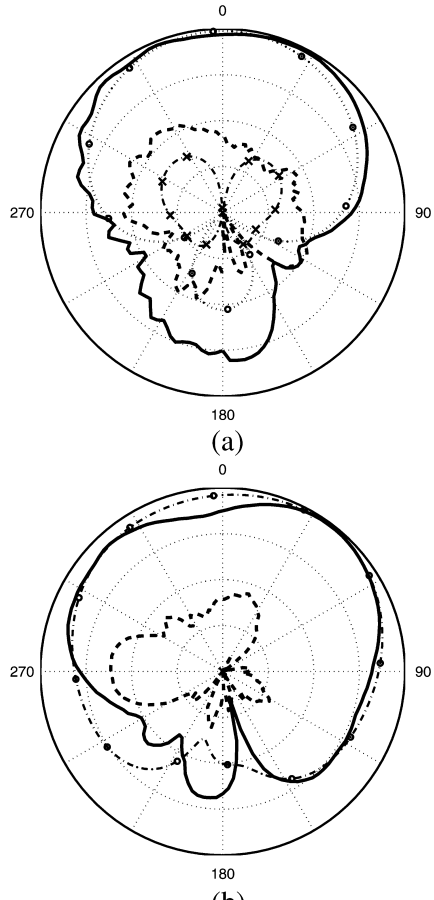

Fig. 7. Radiation pattern at 5.725 GH, (a) xy-plane, (b) xz- plane,—: measured E_θ, - - -: measured E_ϕ, -o-: simulated E_θ, -×-: simulated E_ϕ, 10-dB per division on radials, all parameters are the same as in Fig. 5.

Figs. 6 and 7 show the radiation patterns on xy- and xz-planes at 4.98 GHz and 5.725 GHz, respectively. At $f = 4.98$ GHz, the half-power beamwidth (HPBW) of E_θ pattern on the xy-plane is about 90° ($-45° \leq \phi \leq 45°$), and the E_ϕ pattern is 14 dB lower than the E_θ pattern over the beamwidth. The gain is about 5.6 dBi at $\phi = 0°$, and the front-to-back ratio is about 20 dB. At $f = 5.725$ GHz, the HPBW of E_θ pattern on the xy-plane is about 71° ($-40° \leq \phi \leq 31°$), and the E_ϕ pattern is 25 dB below the E_θ pattern over the beamwidth. The gain is 3.5 dBi at $\phi = 0°$, which is lower than that at $f = 4.98$ GHz because the beam of the E_θ pattern on the xz-plane is tilted to $\theta = 36°$, at which the gain is 7.2 dBi. The front-to-back ratio is about 10 dB. For WLAN applications, for example, this DR antenna can be mounted on the wall with the $\hat{z}$-axis pointing to ceiling, providing a broadside radiation pattern with vertical polarization on the xy-plane in front of the wall.

IV. Conclusion

A wideband DR with a tunnel is proposed, which has a 20% impedance bandwidth (4.76–5.86 GHz), wide enough to cover the WLAN 802.11a band. It is achieved by merging the bands of TE^y_{111} and modified TE^y_{112} modes. The electric field distribution of the TE^y_{112} mode is significantly modified by the tunnel. A broadside radiation pattern of vertical polarization on the xy-plane is achieved over the bandwidth.

References

[1] A. A. Kishk, B. Ahn, and D. Kajfez, "Broadband stacked dielectric resonator antenna," *Electron. Lett.*, vol. 25, no. 18, pp. 1232–1233, Aug. 1989.

[2] R. Chair, A. A. Kishk, K. F. Lee, and C. E. Smith, "Broadband aperture coupled flipped staired pyramid and conical dielectric resonator antennas," in *Proc. IEEE APS Int. Symp.*, June 2004, vol. 2, pp. 20–25.

[3] K. Pliakostathis and D. Mirshekar-Syahkal, "Stepped dielectric resonator antennas for wideband applications," in *Proc. IEEE APS Int. Symp.*, Jun. 2004, vol. 2, pp. 1367–1370.

[4] T. A. Denidni, Q. Rao, and A. R. Sebak, "Broadband L-shaped dielectric resonator antenna," *IEEE Antennas Wireless Propag. Lett.*, vol. 4, pp. 453–454, 2005.

[5] R. Chair, A. A. Kishk, and K. F. Lee, "Wideband low profile eye shaped dielectric resonator antennas," in *Proc. IEEE APS Int. Symp.*, Jul. 2005, vol. 3A, pp. 582–585.

[6] Y.-D. Kim, M.-S. Kim, and H.-M. Lee, "Internal rectangular dielectric resonator antenna with broadband characteristic for IMT-2000 handset," in *Proc. IEEE APS Int. Symp.*, Jun. 2002, vol. 3, pp. 22–25.

[7] S. M. Deng, C. L. Tsai, S. F. Chang, and S. S. Bor, "A CPW-fed suspended, low profile rectangular dielectric resonator antenna for wideband operation," in *Proc. IEEE APS Int. Symp.*, Jul. 2005, vol. 4B, pp. 242–245.

[8] M. Verplanken and J. V. Bladel, "The magnetic-dipole resonances of ring resonators of very high permittivity," *IEEE Trans. Microw. Theory Tech.*, vol. 27, pp. 328–333, Apr. 1979.

[9] A. Ittipiboon, A. Petosa, D. Roscoe, and M. Cuhaci, "An investigation of a novel broadband dielectric resonator antenna," in *Proc. IEEE APS Int. Symp.*, Jul. 1996, vol. 3, pp. 2038–2041.

[10] B. Li and K. W. Leung, "A wideband strip-fed rectangular dielectric resonator antenna," in *Proc. IEEE APS Int. Symp.*, Jul. 2005, vol. 2A, pp. 172–175.

[11] Y. M. M. Antar, D. Cheng, G. Seguin, B. Henry, and M. G. Keller, "Modified waveguide model (MWGM) for rectangular resonator antenna (DRA)," *Microw. Opt. Tech. Lett.*, vol. 19, no. 2, pp. 158–160, Oct. 1998.